JOURNAL OF APPLIED ELECTROCHEMISTRY 23 (1993) 364–370

Nucleation and growth of zinc electrodeposits on a polycrystalline zinc electrode in the presence of chloride ions

M. SÁNCHEZ CRUZ, F. ALONSO, J. M. PALACIOS

Instituto de Química Física 'Rocasolano', C.S.I.C., C. Serrano, 119, 28006 Madrid, Spain

Received 12 November 1992; revised 19 August 1992

The kinetics of the nucleation and growth of zinc on a zinc electrode in 0.1 M $ZnCl_2$ has been studied by the potential step technique. Four supporting electrolytes were used: 0.5 M NaCl, 1 M NaCl, 3 M NaCl and 1 M $NaClO_4$. The current decays to a minimum, after which it rises to a maximum and then decreases again. The initial part of the transient, up to the current minimum, includes the double layer charging and the initial nucleation and growth of zinc. The rising part of the transition curve, from the current minimum to the maximum, follows the model of progressive nucleation and diffusion-controlled, hemispherical three dimensional growth. The steady state nucleation rate and the nuclear number density increase with the overpotential and with the NaCl concentration. The results point to a direct involvement of zinc chlorocomplexes in the electrodeposition process.

1. Introduction

The intial stage of zinc electrocrystallization on zinc has been little studied. However, there is an abundance of studies on the several factors affecting the quality of zinc electrodeposits, e.g. morphology and crystallographic orientation of the substrate, impurities, additives, experimental procedure. In the deposition at low overpotentials of zinc on zinc single crystals in 3 M $ZnCl_2$, the reaction kinetics, as well as the morphology of the deposit and the type of growth, depend on the crystallographic orientation of the electrode [1]. A superimposed alternating current noticeably increases the rate of zinc nucleation on polycrystalline zinc in zinc chloride solution, thereby favouring homogeneity of the deposits [2].

Both the nucleation and the deposition kinetics are extremely sensitive to the presence in the solution of impurities and organic and inorganic additives in very low concentrations. The effect of the additives is complex and variable. In general, additives modify the zinc deposition overvoltage and, leaving aside other kinetic complications, they change the ratio of the nucleation rate to the growth rate [3, 4]. So, using very short potentiostatic pulses, it has been found that at low overpotentials the addition of 50 p.p.b. Sn increases the number of zinc nuclei on a vitreous carbon electrode [5]. At higher overpotentials all the zinc nuclei reach a similar size, which shows that nucleation is instantaneous.

Obviously the nature of the substrate has an important effect on zinc nucleation. The nucleation overpotential on cathodes of vitreous carbon (VC), aluminium and lead, measured as the width of the hysteresis loop in the voltammetric curves, increases in the order VC < Al < Pb [6]. The slopes of the current–time curves at potentials near the crossover point show the opposite behaviour, this effect being still noticeable even at fairly high zinc coverages.

Despić and Pavlovic [7] studied the initial step of the electrodeposition of zinc on Pt, Au and graphite electrodes, and found that only those substrates, like graphite, to which the electrodeposited zinc atoms do not adhere strongly, show a significant nucleation effect. With graphite nucleation and growth are a 3D instantaneous process. The influence of the substrate on the growth mechanism remains at higher than monoatomic coverages.

The study of McBreen and Gannon [8] of the initial step of zinc electrodeposition on vitreous carbon in 3 M $ZnCl_2$ and 3 M $ZnBr_2$ is especially interesting. They found that the nucleation overpotential is lower in the first than in the second electrolyte, probably owing to the fact that the stability constant of zinc bromocomplexes is lower than that of zinc chlorocomplexes. In both solutions the mechanism is one of instantaneous nucleation and 3D growth under kinetic control.

In this work we have studied the electrochemical nucleation of zinc on a zinc electrode, and the effect of the chloride concentration on this process.

2. Experimental details

The working electrode was a zinc cylinder (Puratronic, 99.999% pure, from Alfa Ventron) embedded in Araldite epoxy resin, with an exposed area of 0.128 cm^2. The electrolytic cell has been described previously [9]. A vitreous carbon sheet, 3 cm^2 in area (one side), and an ultrapure zinc wire, 0.2 cm in diameter, were used as auxiliary and reference electrodes, respectively. The rest potential of the zinc electrode in the different solutions was also measured with respect to an SCE electrode.

0021-891X

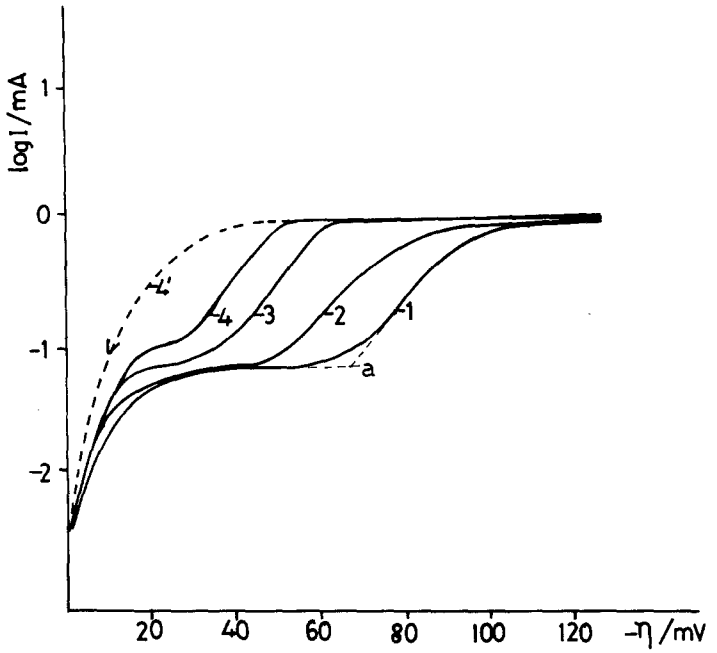

Fig. 1. Cathodic voltammograms at 1 mV s^{-1} of a zinc electrode in a 0.1 M $ZnCl_2$ solution, in the presence of the following supporting electrolytes: 0.5 M NaCl (curve 1); 1 M $NaClO_4$ (curve 2); 1 M NaCl (curve 3); and 3 M NaCl (curve 4). The rest potential against SCE of the zinc electrode was: (1) −1040; (2) −1006; (3) −1042; and (4) −1053 mV.

Special attention was devoted to the preparation of the zinc electrode, in order to ensure a good reproducibility of the experiments, which is crucial in comparative measurements. Before each experiment the electrode was successively polished in a Buehler 'Minimet' Polisher/Grinder with no. 600 silicon carbide paper and with increasingly fine alumina powder down to 0.05 μm on Microcloth, then rinsed thoroughly with ultrapure water, and finally cleaned in an ultrasonic bath.

The solutions were prepared with Milli-RO + Milli-Q (Millipore, Bedford, Mass.) ultrapure water and $ZnCl_2$, NaCl and $NaClO_4$ analytical reagents (AR) from Merck. The solution pH was always adjusted to 2.6 with HCl. All solutions were deoxygenated with nitrogen before use.

Four different solutions, with the same concentration of $ZnCl_2$ (0.1 M) and, respectively, with (1) 0.5 M NaCl, (2) 1 M NaCl, (3) 3 M NaCl, and (4) 1 M $NaClO_4$ as supporting electrolytes, were used.

All cyclic voltammetric and potential step experiments were performed with a Solartron 1286 Electrochemical Interface with ohmic drop compensation, a Hewlett-Packard 'Color-Pro' plotter, a YEW-3033 *X–Y–t* recorder and a digital storage oscilloscope Trio MS-1650 A.

3. Results

3.1. *Voltammetric behaviour*

In Fig. 1 typical cathodic voltammograms starting at $\eta = 0$ mV in quiescent solution are shown for the four supporting electrolytes used. The values of the rest potentials (with respect to SCE), included in the legend to Fig. 1, clearly show the presence in NaCl solutions of zinc chlorocomplexes.

The current grows sharply at a given, critical value of η (point *a* in the example of curve 1 in Fig. 1). The hysteresis loop between the descending and ascending branches of the voltammogram (curve 4′ in Fig. 1) is due to the increase of the electroactive area of the electrode and to the nucleation process which, in the first sweep and at low overpotentials, controls the global electrodeposition kinetics. The hysteresis loop is no longer present in successive sweeps.

The overpotential at which the diffusion-limited current is reached decreases with increasing NaCl concentration, which shows that chloride ions increase the electrodeposition rate.

It is to be noted that the curve in 1 M $NaClO_4$ (curve 3, Fig. 1) has an intermediate position between those in 0.5 M and 1 M NaCl.

3.2. *Current–time transients*

Negative potentiostatic pulses from $\eta = 0$ mV to several overpotential values, usually higher than −50 mV, were carried out in quiescent solutions. Smaller overpotentials were not used because they led to inordinately long transients. Possibly a given degree of supersaturation is required to initiate nucleation. In Fig. 2 a typical I against t transient is given. The pertinent parameters, extracted from the transients for the four solutions, are collected in Table 1. Initially the current grows sharply, after which it decreases to a minimum, I_0, at time t_0, forming a small peak, sometimes not well defined. Then the current increases to a maximum, I_m, at the time t_m, after which it decreases again.

In general the values of I_0 are fairly high, and tend to increase with the overpotential, which points to the formation of growth centres at this initial stage. Effectively, the electric charge, Q_0 (determined with the

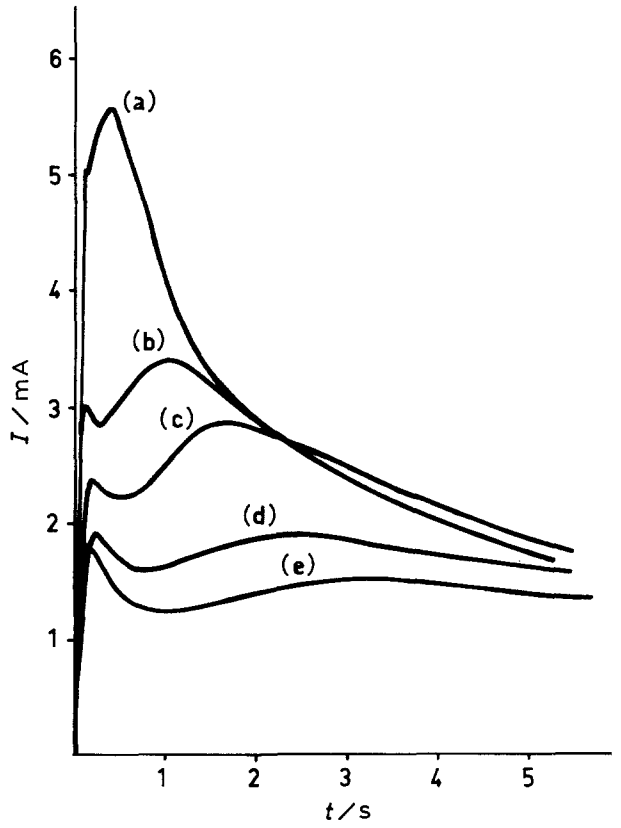

Fig. 2. Potentiostatic I–t transients of a zinc electrode in 0.1 M $ZnCl_2$ + 3 M NaCl solution, recorded after stepping the potential from $\eta = 0$ to: (a) −100; (b) −90; (c) −70; (d) −50; and (e) −40 mV.

digital storage oscilloscope), consumed up to t_0, is always more than one order of magnitude higher than that required to deposit a compact zinc monolayer (about 520 μC cm^{-2}), and decreases upon increasing the overpotential and the NaCl concentration. It is clear that the process of nucleation and growth starts before the time t_0 is reached, and overlaps the double-layer charging, which usually lasts a fraction of a millisecond.

The electric charges, Q_m, associated with the current maximum, and calculated as the charge consumed from time t_0 to time t_m, also decrease with increasing overpotential and NaCl concentration, due, in both cases, to the 'contraction' of the time scale. The value of Q_m corresponds to several zinc monolayers, from 10 to 150.

The theoretical interpretation of the current transient in terms of a given model of nucleation and growth [10, 11] requires a determination of the value of the exponent n in the expression I against t^n which describes the rising branch of the curve at times $t < t_m$. The value of n (1/2; 1; 2/3; 2; and 3) depends on the geometry of the growth centre (cylindrical, circular cones, hemispherical), on the nucleation type (instantaneous, progressive), and on the type of growth (bidimensional, tridimensional) under kinetic or diffusion control [12, 13].

For the rising section of the transients the current values are taken as $I' = I - I_0$. Plotting I' against t^n for different n values a linear relationship is obtained for $n = 1$. For $n = 3/2$ the relationship is also linear, but for a shorter time range, as shown in Fig. 4. Obviously the corresponding nucleation-growth model is very different: while a value of $n = 1$ is compatible with an instantaneous nucleation followed by 2D growth of cylindrical centres under kinetic control [10, 14–16], a value of $n = 3/2$ is compatible with a diffusion-controlled three dimensional growth of hemispherical nuclei with progressive nucleation [17, 18]. In this last case the net current can be expressed as:

$$I(t) = \frac{2}{3} zF\pi AN_\infty (2Dc)^{3/2} \left[\frac{M}{\rho}\right]^{1/2} t^{3/2} \qquad (1)$$

where z is the valence of Zn (2), A the nucleation rate per active site (s^{-1}), N_∞ the number density of active sites for nucleation (cm^{-2}), D the diffusion coefficient (cm^2 s^{-1}), c the zinc bulk concentration (mol dm^{-3}, i.e. M), M the atomic mass of zinc (65.38 g mol^{-1}), and ρ the density of zinc (7.14 g cm^{-3}).

It is evident that in order to discriminate between the two models of nucleation and growth the analysis of the current transients must be complemented with additional information on the kinetics of the deposition process and on the geometry of the growth centres. The SEM micrographs of the electrode surface at short polarization times (Fig. 5a, b and c) reveal the presence of growth centres of different sizes, whose number and size increase with time. At the higher magnification (Fig. 5b) the hemispherical form of a growth centre can be clearly appreciated.

Further deposition experiments with potentiostatic pulses were carried out with a zinc rotating disc electrode at 3000 r.p.m. under otherwise identical conditions. The current transients are markedly affected: the maximum disappears, and at long times the current tends towards a stationary value (Fig. 3).

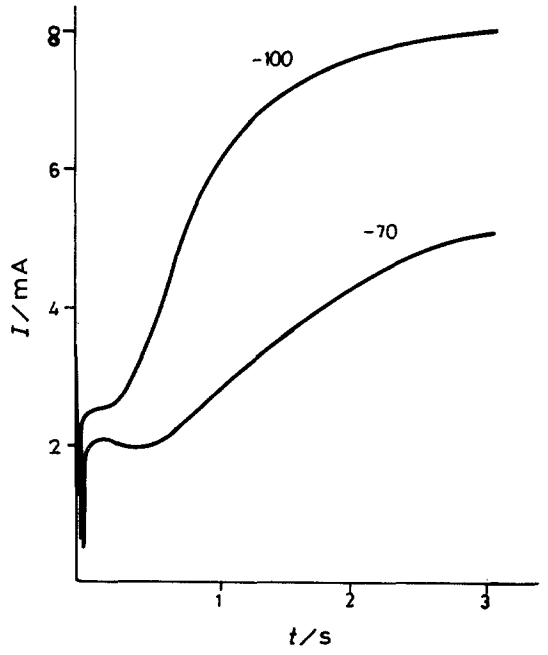

Fig. 3. Representative I–t transient of zinc electrodeposition on a rotating (at 3000 r.p.m.) zinc electrode at $\eta = -100$ mV and $\eta = -70$ mV 0.1 M $ZnCl_2$ + 3 M NaCl solutions.

Table 1.

Supporting electrolyte	$-\eta$ /mV	$10^2 i_m$ /A cm^{-2}	$10^2 i_o$ /A cm^{-2}	t_m /s	t_o /s	$10^3(di/dt^{3/2})$ /A cm^{-2} s$^{-3/2}$	$10^{-5} A_\infty$ /cm^{-4} s^{-1}	$10^{-5} N$ /cm^{-2}	$10^4(i_m^2 t_m)$ /A^2 cm^{-4} s
0.5 M NaCl	50	0.57	0.33	18.20	2.75	0.1	0.011	0.038	5.9
	80	1.30	0.96	4.34	1.10	1.5	0.17	0.24	7.3
	100	1.67	0.78	3.30	0.80	4.8	0.53	0.46	9.2
	120	2.31	0.74	2.00	0.52	9.5	1.10	0.78	10.6
	130	3.13	1.82	0.20	0.20	41.5	4.60	1.63	9.3
1 M NaCl	50	1.08	0.52	6.10	1.50	1.1	0.12	0.21	7.1
	60	1.18	0.66	5.50	1.17	1.5	0.16	0.24	7.6
	70	1.38	0.79	4.20	0.42	5.85	0.65	0.61	8.0
	100	2.50	1.50	1.41	0.26	25.0	2.80	1.22	8.8
	130	5.55	4.65	0.21	0.04	250.0	27.70	2.40	6.5
3 M NaCl	40	1.20	0.99	3.3	1.00	1.6	0.17	0.20	4.7
	50	1.48	1.25	2.4	0.74	2.6	0.29	0.23	5.2
	70	2.24	1.72	1.74	0.52	7.3	0.81	0.56	8.7
	90	2.63	2.23	1.02	0.26	22.0	2.40	0.64	7.7
	100	4.34	3.94	0.37	0.13	58.6	6.50	0.08	6.9
1 M $NaClO_4$	80	1.09	0.49	7.75	0.86	1.6	0.18	0.34	9.2
	100	1.26	0.93	3.20	0.60	2.6	0.29	0.25	5.1
	130	2.54	1.60	1.10	0.22	34.4	3.80	1.50	7.1
	140	3.36	2.15	0.57	0.15	127.0	14.0	2.40	6.4

In the rising section the slope is higher, and at the beginning of the transition there appears a wave, probably related with the initial transition peak of Fig. 2. The nature of this initial process has not been studied here.

Both the SEM micrographies and the rotating disc experiments indicate that the nucleation is progressive and three-dimensional, and that the growth of the nuclei is diffusion-controlled.

An analysis of the long-time falling transients (Fig. 2) for higher overpotentials in terms of the Cottrell equation,

$$I = zD^{1/2}[Zn^{2+}]\pi^{-1/2}t^{-1/2} \qquad (2)$$

yields $D = (8.8 + 0.2) \times 10^{-6}$ cm^2 s^{-1} for the Zn^{2+} in NaCl solutions, and $(7.9 + 0.1) \times 10^{-6}$ cm^2 s^{-1} in 1 M $NaClO_4$ solution. These values are in good agreement with those found by other authors using different experimental techniques [19–21]. The calculations were carried out assuming that the concentration of the Zn^{2+} ion was 0.1 M, i.e. neglecting the formation of chlorocomplexes in the NaCl solutions. Effectively, the constancy of the diffusion-limited current in the voltammetric curves (Fig. 1) shows that the mass transfer conditions are the same in all cases.

It is well known that the higher complexes of zinc ($ZnCl^{3-}$, $ZnCl^{4-}$) are less hydrated, and therefore should diffuse more rapidly, than the more hydrated Zn^{2+} and $ZnCl^{+}$ ions. It must be taken into account that the above calculated diffusion coefficient is a composite coefficient, since it includes the negative

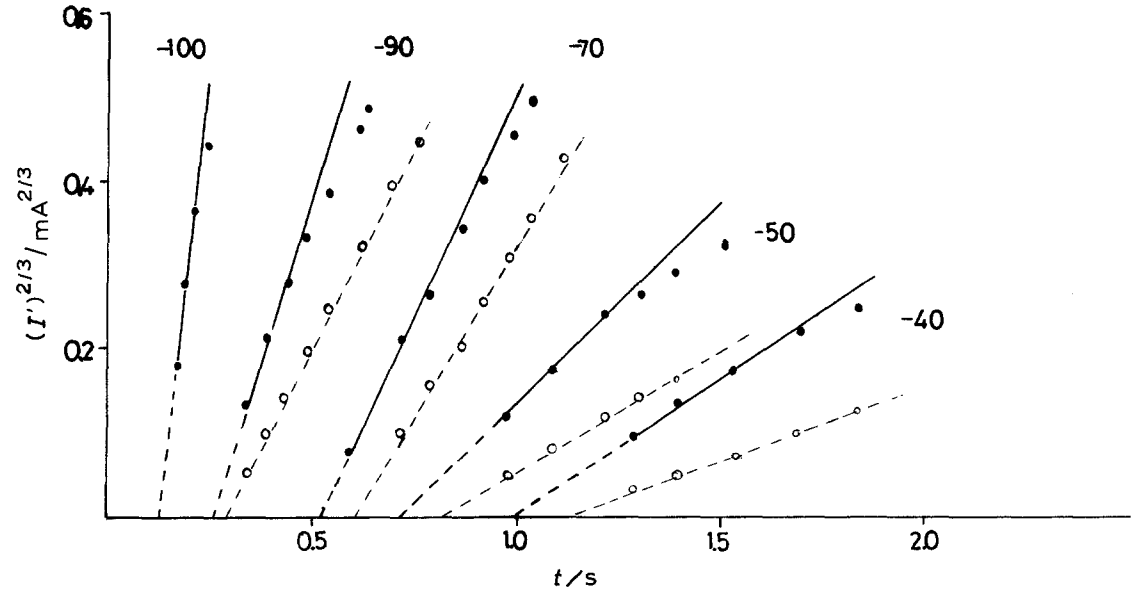

Fig. 4. $(I')^{2/3}$ against (——) and I' against t (- - -) plots of the rising section of the transients in Fig. 2. Extrapolation to $I' = 0$ yields the delay time, t_0.

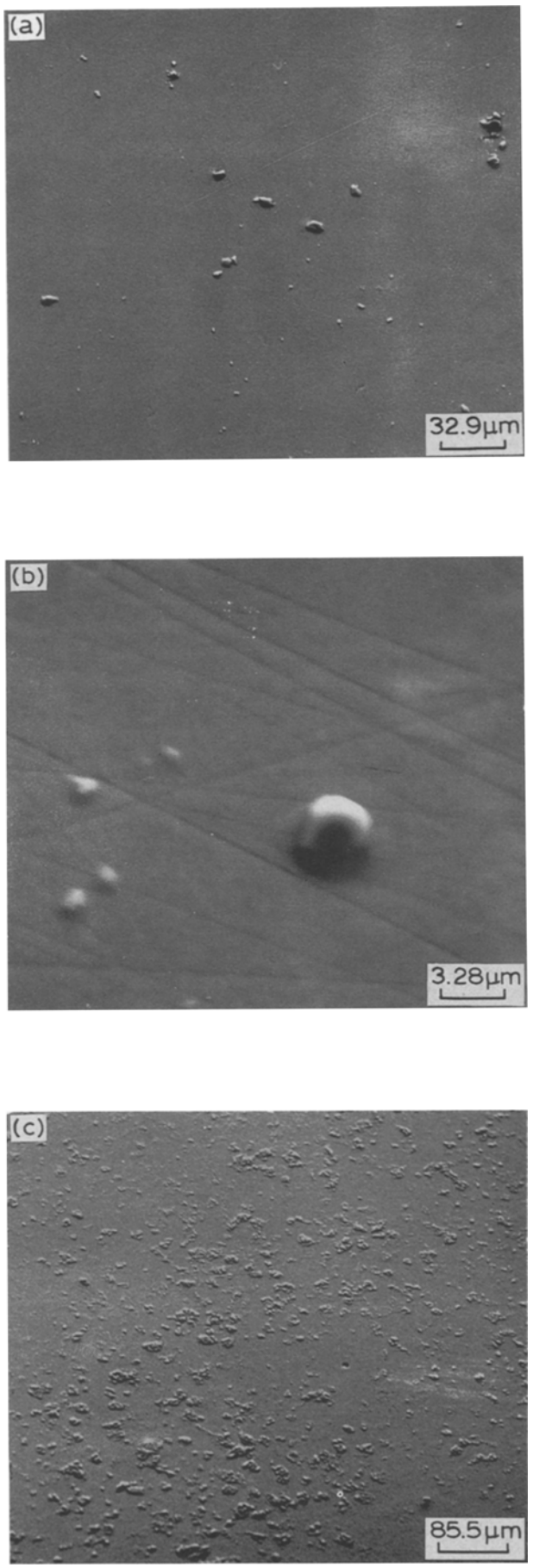

Fig. 5. SEM micrograph of zinc electrodeposited on a zinc electrode at $\eta = -70$ mV in 0.1 M $ZnCl_2$ + 1 M NaCl solution. (a) after 1.8 s; (b) same as (a) but at a higher magnification; (c) same as (a) but after 2.6 s.

contribution of the migration of the negative chlorocomplexes and the effect of cation hydration, which changes with its concentration. The influence of these effects increases with $ZnCl_2$ concentration and with the stoichiometric ratio of chloride to zinc ion. In 0.1 M $ZnCl_2$ solutions and in the 0.5–3 M NaCl concentration range all zinc chlorocomplexes coexist, possibly with $ZnCl^+$ and $ZnCl_3^-$ as dominant complex species [21]. Under our experimental conditions no single species is mainly responsible for the global transport process. Besides, it is well known that the reacting complex species is not necessarily the dominant complex species, provided the concentration of the reacting species at the electrode surface is held constant by rapid homogeneous reactions.

From the slopes of the straight sections of the I against $t^{3/2}$ plots at short times the value of the steady state nucleation rate, AN_∞, was calculated. Table 1 shows that this value increases with overpotential and with NaCl concentration.

From the values of i and t at the maximum of the transient the product $(i_m^2 t_m)$ can be calculated as a diagnostic parameter for checking if the nucleation process is continuing or has stopped. Under our experimental conditions ($D = 8.8 \times 10^{-6}\,cm^2\,s^{-1}$, $c = 0.1$ M) the theoretical value of the product $(i_m^2 t_m)$ is 5.3×10^{-4} and $8.5 \times 10^{-4}\,A^2\,cm^{-4}\,s$ for instantaneous and progressive nucleation, respectively. Some of the values in Table 1 lie between these two values. The too low values of the product at low overpotentials can be attributed to insufficient precision in the determination of t_m.

The above problem makes it necessary to analyse the current transient at longer times, but also preceding the maximum. The plot of $\log I'$ against t' (both magnitudes in the corrected scale in order to increase precision) shows two linear segments, with slopes close to 1.5 and 0.5, respectively (Fig. 6). This behaviour is frequently observed in the electrodeposition of metals under diffusion control [12, 22], and indicates that the nucleation is not progressive over the whole transient, but that at a certain time it changes from progressive to instantaneous.

The rising middle section of the current transient was analyzed according to the equation

$$I = zF\pi(2DC)^{3/2}\left[\frac{M}{\rho}\right]^{1/2} Nt^{1/2} \qquad (3)$$

for diffusion-controlled, hemispherical, three-dimensional growth with instantaneous nucleation. In this way the values of the nuclear number density, N, given in Table 1, were evaluated.

The value of the ratio $[AN_\infty/N]$, i.e. the ratio between the number of progressively nucleated sites to that of instantaneously nucleated sites, gives an indication of the nucleation rate constant. The increase in this ratio with the overpotential and with the NaCl concentration (Fig. 7) suggests that the incorporation of the zinc atoms to the growth centre takes place

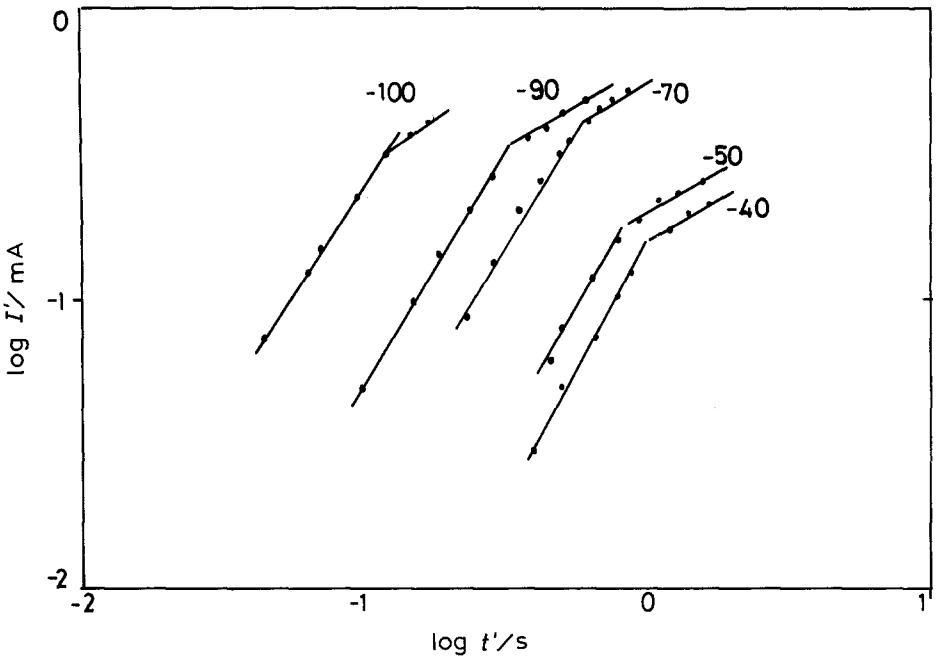

Fig. 6. Plot of $\log I'$ against $\log t'$ of the rising part of some transients, at the overpotentials (in mV) indicated, in 0.1 M + 3 M solutions.

directly from the bulk, and not through an adsorption step. By contrast Mostany *et al.* [23] have found that in the nucleation of lead (Pb) on a vitreous carbon electrode the density of active sites for nucleation is increased by the presence of Cl^- and Br^- ions. This effect was attributed to the adsorption on the electrode of halide ions and/or of the PbX_n^{2-n} complex species, which promote the creation of new nucleation sites.

4. Conclusions

It is improbable that the influence of the NaCl concentration is due to kinetic changes produced by adsorbed Cl^- ions, since no significant change in adsorption should be observed at the high NaCl concentrations used. It cannot be due to changes in the ionic strength either, since the data of Fig. 7 for the supporting

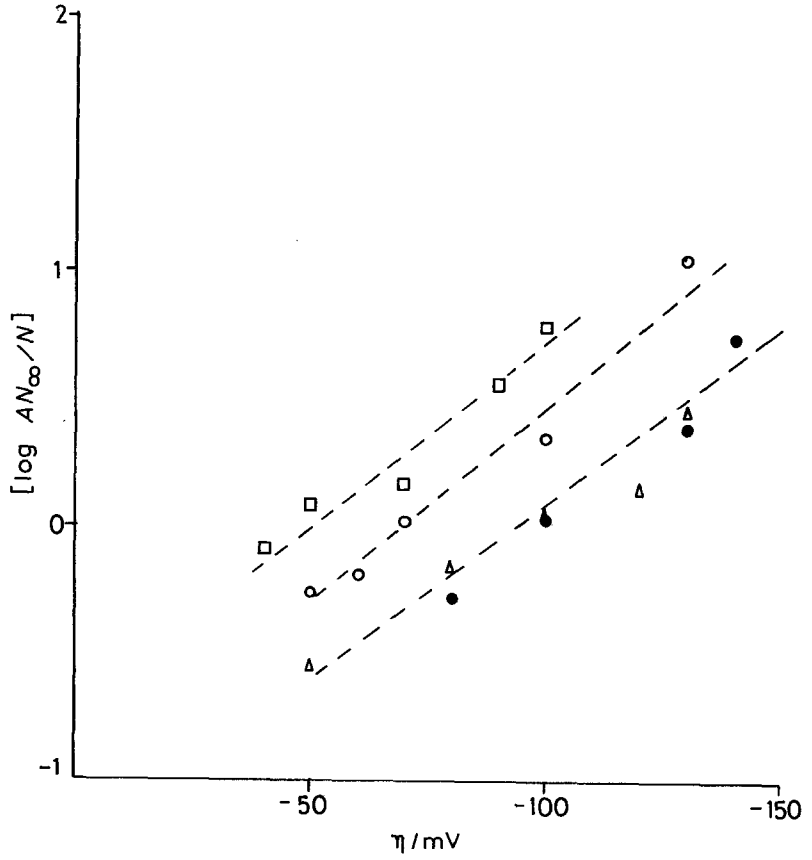

Fig. 7. Overpotential dependence of the AN_∞/N ratio for the zinc electrodeposition in 0.1 M $ZnCl_2$ solution with the following supporting electrolytes: (□) 3 M NaCl; (○) 1 M NaCl; (△) 0.5 M NaCl; and (●) 1 M $NaClO_4$.

electrolytes 0.5 M NaCl and 1 M $NaClO_4$, i.e. at different ionic strengths, coincide within experimental error.

According to the results presented here, the electrodeposition of zinc on zinc follows an electrocrystallization model of 3D growth under diffusion control, with a nucleation that is progressive at short times and instantaneous at longer times. With increasing overpotential and NaCl concentration the product (AN_∞) increases more rapidly than does N, which shows that the predominance of the progressive over the instantaneous nucleation is a function of these two parameters.

It is reasonable to assume that the effect of the NaCl concentration is related to the increase in the degree of complexation and stability of zinc chlorocomplexes [21, 24]. The direct involvement of zinc chlorocomplexes in the electrodeposition process has been pointed out by other workers [25, 26], although under different experimental conditions.

Acknowledgements

This work was performed under Project No. PA86–0440 of the Spanish CICYT. The financial support of the firm Técnicas Reunidas, S.A. is gratefully acknowledged.

References

[1] J. McBreen and E. Gannon, *J. Electrochem. Soc.* **133** (1986) 2047.
[2] D.-T. Chin and S. Venkatesh, *ibid.* **128** (1981) 1439.
[3] D. J. Mackinnon and J. M. Brannen, *J. Appl. Electrochem.* **12** (1982) 21.
[4] D. J. Mackinnon, J. M. Brannen and R. M. Morrison, *ibid.* **12** (1982) 39.
[5] A. C. Beshore, B. J. Flori, G. Schade and T. J. O'Keefe, *ibid.* **17** (1987) 765.
[6] T. Biegler, *in* 'Application of polarization measurements in metal deposition', (edited by I. H. Warren), Elsevier, Amsterdam (1984).
[7] A. R. Despic and H. G. Pavlovic, *Electrochim. Acta* **27** (1982) 1539.
[8] J. McBreen and E. Gannon, *J. Electrochem. Soc.* **130** (1983) 1667.
[9] M. Sánchez Cruz, F. Alonso and J. M. Palacios, *J. Appl. Electrochem.* **20** (1990) 611.
[10] M. Fleischmann and H. R. Thirsk, *in* 'Advances in Electrochemistry and Electrochemical Engineering', (edited by P. Delahay), Vol. 3, Wiley Interscience, New York (1972).
[11] R. Gref, R. Peat, L. M. Peter, D. Pletcher and J. Robinson, 'Instrumental Methods in Electrochemistry'. Wiley, New York (1985) Ch 9, p. 283.
[12] G. Gunawardena, G. Hills, I. Montenegro and B. Scharifker, *J. Electroanal. Chem.* **138** (1982) 225.
[13] M. R. Thirsk and J. A. Harrison, 'A guide to the study of electrode kinetics', Academic Press, New York (1972).
[14] D. J. Astley, J. A. Harrison and H. R. Thirsk, *Trans. Faraday Soc.* **64** (1968) 192.
[15] A. Bewick, M. Fleischmann and H. R. Thirsk, *Trans. Faraday Soc.* **58** (1962) 2000.
[16] R. D. Armstrong, M. Fleischmann and H. R. Thirsk, *J. Electroanal. Chem.* **11** (1966) 208.
[17] G. J. Hills, D. J. Schiffrin and J. Thompson, *Electrochim. Acta* **19** (1974) 657.
[18] B. Scharifker and G. Hills, *ibid.* **28** (1983) 879.
[19] J. T. Kim and J. Jorné, *J. Electrochem. Soc.* **127** (1980) 8.
[20] D. Loftus, J. Roberts, R. Weaver, S. Leach and L. Nanis, *ibid.* **130** (1983) 332.
[21] W. C. Hsie and J. R. Selman, *Electrochim. Acta* **30** (1985) 1381.
[22] G. Gunawardena, G. J. Hills and I. Montenegro, *J. Electroanal. Chem.* **184** (1985) 371.
[23] J. Mostany, J. Parra and B. R. Scharifker, *J. Appl. Electrochem.* **16** (1986) 333.
[24] E. Skou, T. Jacobsen, W. van der Hoeven and S. Atlung, *Electrochim. Acta* **22** (1977) 169.
[25] O. V. Larinov and Ya. V. Duzdin, *Elektrokhim.* **8** (1972) 1818.
[26] Ya. D. Zynter and I. A. Kravchova, *ibid.* **11** (1975) 1219.